

FEASIBILITY STUDY OF AN ULTRAFAST ELECTRON DIFFRACTION SYSTEM IN NSRRC

P. Wang, K.C. Leou, Department of Engineering and System Science, NTHU, Hsinchu, Taiwan
 A.P. Lee, N.Y. Huang, W.K. Lau, NSRRC, Hsinchu, Taiwan

Abstract

It has been suggested that the MeV beam generated from a laser-driven photo-cathode rf gun can be used for ultrafast electron diffraction (UED). The feasibility of operating the NSRRC photo-cathode rf gun system for ultrashort bunch generation is being investigated. The results of space-charge tracking calculations show that a low emittance, few hundred femtoseconds MeV beam with reasonable bunch charge can be generated for single shot UED experiments. In this report, a preliminary design of this UED system will be discussed.

INTRODUCTION

Ultrafast dynamics of matter in atomic-scale resolution can be investigated with short electron pulses. The idea of using photo-cathode rf guns to produce MeV femtosecond electron beams for ultrafast electron diffraction (UED) experiments is first proposed by X.J. Wang in Brookhaven National Laboratory [1]. It has been demonstrated experimentally the feasibility to employ such gun to obtain single shot electron diffraction pattern of aluminium foil at SLAC [2]. A number of UED systems are then developed or under development worldwide [3-5].

A 2998 MHz, 1.6-cell photo-cathode rf gun system has been developed in NSRRC [6]. The rf gun cavity has been fabricated with full-cell to half-cell field ratio is adjusted to 1 during bench test. This cavity has been powered up to ~60 MV/m. Normalized emittance of the electron beam driven by Gaussian laser pulses is about 5.5 mm-mrad at 250 pC as measured with multi-slits. An ultrafast 266 nm laser with adjustable pulse duration is used to produce photoelectrons from the Cu cathode in the rf gun cavity. The shortest pulse duration generated from the laser system is 100 fs FWHM. It is under consideration to use such beam for setting up a UED system for time-resolved research. In this report, we studied the beam dynamics of a short electron pulse in the rf gun and in the drift section which is located at downstream with space-charge tracking simulation. Application of solenoid magnetic field for limiting the beam from excessive divergence and insertion of a collimation pinhole are possible to improve the spatial resolution of diffraction patterns.

SPATIAL RESOLUTION

A typical setup for UED system with photo-cathode rf gun that delivers few MeV electron beam is shown in Fig. 1. To achieve good spatial quality of diffraction patterns, the resolving power of UED system must be carefully considered [3]. It is defined as $r = R/\Delta R$, where R is the radius of the diffraction rings on detector and ΔR is the

width of the diffraction rings. Based on simple geometry, the resolving power can be derived as

$$r = \frac{h}{2m_0cd} \frac{\sigma_{x0}}{\varepsilon_n}$$

where σ_{x0} is the beam size measured at longitudinal position of the sample, ε_n the normalized beam transverse emittance and d the distance between lattice. A pinhole is used for selection of low emittance beam while maintaining reasonable number of electrons on the screen after the sample (i.e. $\sim 10^6$ - 10^7). It has been suggested that r has to be larger than ten for good quality of diffraction patterns [3].

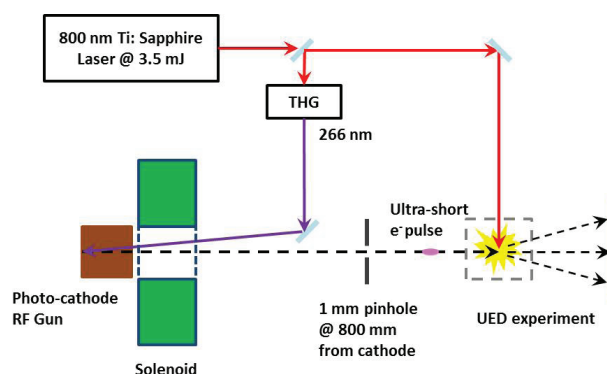


Figure 1: Typical UED system with relativistic electron beam from photo-cathode rf gun.

GENERATION AND PROPAGATION OF FEMTOSECOND BEAM

The properties of the MeV beam from the photo-cathode rf gun are in general depend on bunch charge, laser pulse shape, laser injection phase, pulse shape and stability etc., simulation study with space charge tracking code GPT [7] has been carried out to search for best operation condition at 100 fsec initial bunch length. Initial beam size on cathode is chosen at 0.5 mm.

The maximum energy of electron beam that be generated from the gun when the accelerating gradient is operated at 55 MV/m is about 2.85 MeV according to the simulation result. Fig. 2 shows how the average beam energy changes with laser injection phase. The zero phase is defined at -90° from rf crest. To get high beam energy at fixed accelerating gradient, the injection phase is usually set within the range 0 - 25° . Beam energy rolls off beyond 25° .

Content from this work may be used under the terms of the CC BY 3.0 licence (© 2014). Any distribution of this work must maintain attribution to the author(s), title of the work, publisher, and DOI.

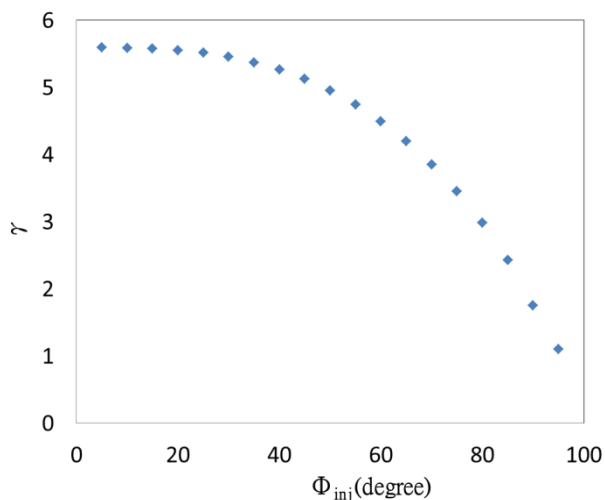


Figure 2: Calculated Lorentz factor (averaged over the whole bunch) of a reference electron in the beam as a function of laser injection phase.

Obviously, distributions of macroparticles in the transverse and longitudinal phase spaces depend upon injection phase. However, in the region of 0-25°, the distributions of macroparticles in phase space are very much similar. Typical in the interested range of injection phase (0-25°) are shown in Fig. 3. For a beam with normalized emittance ϵ_n , resolving power depends on divergence at the location of the sample. It is important to focus the beam with solenoid magnetic field to limit the increase in beam size along the downstream straight section.

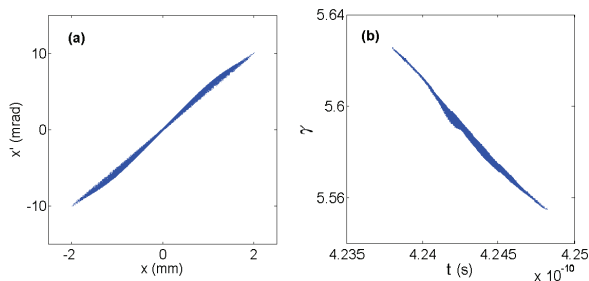


Figure 3: (a) The transverse phase space distribution of electrons at gun exit. (b) The longitudinal phase space distribution of electrons at gun exit.

In longitudinal phase space, as shown in Fig. 3(b), the simulated bunch length at gun exit is 200 fsec. For electrons in the bunch head that have higher kinetic energy, they are moving ahead with respect to the bunch centre as the beam propagates downstream. On the contrary, electrons in the bunch tail that have lower kinetic energy than the average bunch energy are moving behind. As a result, the bunch is lengthened along the drift section at downstream. On the other hand, longitudinal space charge force is going to enhance bunch lengthening as the bunch traverse along the drift section.

BEAM FOCUSING AND COLLIMATION

For the application of UED, the divergence of the beam has to be as small as possible to reach good resolving power. The simulation model used in GPT is based on the setup shown in Fig. 1. The solenoid lens is used for beam focusing. A pinhole will be put just before sample to get much smaller beam size and emittance. In order to reserve enough space for optical mirrors and vacuum components, the distance between cathode and pinhole is set at 80 cm.

The collimation pinhole is important for improvement of spatial resolution [3]. As shown in Fig. 4, outer particles of the beam are removed by insertion of the pinhole.

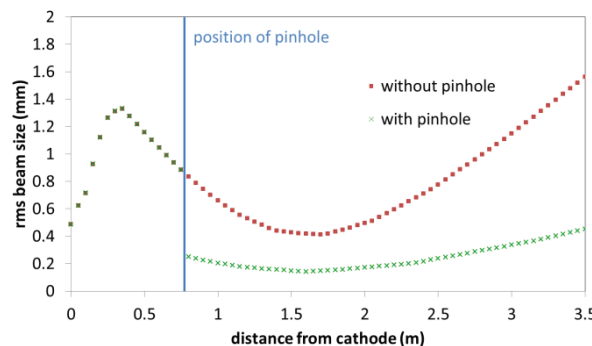


Figure 4: Evolution of beam size along the UED beamline in case without pinhole (red dots) and with pinhole (green).

Much smaller beam size and emittance will promote resolving power obviously. Table 1 illustrates the importance of pinhole installation for improvement of resolving power.

Table 1: Beam Parameters Before and After Pinhole

	Before pinhole	After pinhole
Normalized emittance (mm-mrad)	0.964	0.0933
Beam size (mm)	0.84	0.25
Resolving power	5.25	16.16
Charge (pC)	10	~1

Table 2: Beam Parameters After Pinhole at Various Solenoid Magnetic Field Settings

Solenoid field (gauss)	900	925	975
Normalized emittance (mm-mrad)	0.058	0.067	0.089
Beam size (mm)	0.25	0.24	0.24
Resolving power	25.65	22.00	16.20
Charge (pC)	0.49	0.60	0.99

The beam divergence is pretty much determined by the solenoid magnetic field settings. Since the divergence has to be as small as possible, the magnetic field of the solenoid has to be an appropriate value. Table 2 shows the

resolving power after pinhole compare with different solenoid magnetic power. As the solenoid field get stronger, beam size before pinhole get smaller and more electron pass through pinhole. But at the same time, normalized emittance increase and resolving power decrease. Resolving power > 10 promise a good quality diffraction pattern and particle number have to be maintained enough to get single-shot diffraction pattern ($\sim 10^6$ - 10^7) [3].

Figure 5 shows the changes of rms bunch length with different injection phase. Because the energy of the head of the bunch is higher than the tail, the bunch length will get longer when passing through the drift space. In addition to this, bunch lengthening by the space-charge effect even more important. Figure 5 shows the significant difference between the condition with and without space-charge effect. With the injection phase higher than 50° , the beam energy decrease significant and the space-charge effect even more serious, causing longer bunch lengths.

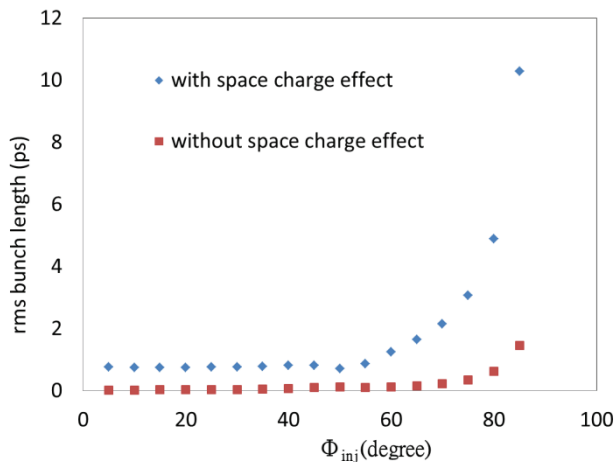


Figure 5: Rms bunch length after pinhole with different injection phase.

In Table 3, the resolving power and charge number of different injection phase is compared and the result shows the resolving power and charge number after pinhole is almost unrelated to the injection phase.

Table 3: Resolving Power and Charge Number With Different Injection Phase

Laser injection phase (degrees)	4	10	14
resolving power	16.2	16.11	16.27
charge number (pC)	0.99	0.98	0.98

CONCLUSION

In summary, the preliminary simulation study suggested a feasible system for femtosecond electron diffraction experiments. Reasonable good resolving power can be achieved by insertion of collimation pinhole and adjustment of solenoid magnetic field for proper beam focusing [3].

To avoid pulse lengthening and beam quality deterioration during beam generation and propagation, it has been suggested to reduce space charge effects by increasing the laser pulse duration at initial stage and perform bunch compression by an alpha magnet located downstream. This method has been proven to be effective for thermionic rf gun [8]. Future study will include the examination of the idea to use similar magnetic bunch compression technique except that we take the advantage of the lower emittance photo-cathode rf gun and beam injection phase selection.

REFERENCES

- [1] X.J. Wang, et al., PAC'03, 420-422 (2003).
- [2] J.B. Hastings et al., Appl. Phys. Lett. 89, 184109 (2006).
- [3] P. Musumeci and R. K. Li, ICFA beam dynamics newsletter No. 59, p.13-33 (2012).
- [4] J. Yang et al., FRXBB01, in proceedings of IPAC 2012.
- [5] R. K. Li et al., Rev. Sci. Instrum. 80, 083303 (2009).
- [6] A.P. Lee et al., THPRO048 in these proceedings.
- [7] General Particle Tracer, <http://www.pulsar.nl/gpt/>
- [8] P. Kung et al., Phys. Rev. Lett. 73, 967 (1994).